

ORIGINAL ARTICLE

Sur1-Trpm4 Cation Channel Expression in Human Cerebral Infarcts

Rupal I. Mehta, MD, Cigdem Tosun, PhD, Svetlana Ivanova, PhD, Natalia Tsybalyuk, MD, Bolanle M. Famakin, MD, Min Seong Kwon, PhD, Rudy J. Castellani, MD, Volodymyr Gerzanich, MD, PhD, and J. Marc Simard, MD, PhD

Abstract

The nonselective monovalent cation channel transient receptor potential melastatin 4 (Trpm4) is transcriptionally upregulated in neural and vascular cells in animal models of brain infarction. It associates with sulfonylurea receptor 1 (Sur1) to form Sur1-Trpm4 channels, which have critical roles in cytotoxic edema, cell death, blood-brain barrier breakdown, and vasogenic edema. We examined Trpm4 expression in postmortem brain specimens from 15 patients who died within the first 31 days of the onset of focal cerebral ischemia. We found increased Trpm4 protein expression in all cases using immunohistochemistry; transcriptional upregulation was confirmed using *in situ* hybridization of *Trpm4* messenger RNA. Transient receptor potential melastatin 4 colocalized and coassociated with Sur1 within ischemic endothelial cells and neurons. Coexpression of Sur1 and Trpm4 in necrotic endothelial cells was also associated with vasogenic edema indicated by upregulated perivascular tumor necrosis factor, extravasation of serum immunoglobulin G, and associated inflammation. Upregulated Trpm4 protein was present up to 1 month after the onset of cerebral ischemia. In a rat model of middle cerebral artery occlusion stroke, pharmacologic channel blockade by glibenclamide, a selective inhibitor of sulfonylurea receptor, mitigated perivascular tumor necrosis factor labeling. Thus, upregulated Sur1-Trpm4 channels and associated blood-brain barrier disruption and cerebral edema suggest that pharmacologic targeting of this channel may represent a promising therapeutic strategy for the clinical management of patients with cerebral ischemia.

Key Words: Cerebral edema, Cerebral infarct, Endothelium, Neuron, Neutrophil, Sulfonylurea receptor 1 (Sur1), Transient receptor potential melastatin 4 (Trpm4).

From the Departments of Pathology (RIM, RJC, JMS), Neurosurgery (SI, NT, MSK, VG, JMS), Neurology (BMF), and Physiology (JMS), University of Maryland School of Medicine, Baltimore, Maryland; and the Department of Molecular Biology and Genetics (CT), Izmir Institute of Technology, Izmir, Turkey.

Send correspondence and reprint requests to: Rupal I. Mehta, MD, Department of Pathology, 22 S. Greene St, NBW81C, Baltimore, MD 21201; E-mail: rmehta@som.umaryland.edu

This work was supported by the National Institute of Neurological Disorders and Stroke (Grant Nos. K08NS089830 and NS061808 to Rupal I. Mehta and J. Marc Simard) and the National Heart, Lung, and Blood Institute (Grant No. HL082517 to J. Marc Simard).

J. Marc Simard holds US patent 7,285,574 (“A novel nonselective cation channel in neural cells and methods for treating brain swelling”). J. Marc Simard is a member of the scientific advisory board of and holds shares in Remedy Pharmaceuticals. Remedy Pharmaceuticals did not support (directly or indirectly) J. Marc Simard on this project. All the other authors declare no conflicts of interest.

INTRODUCTION

Cerebral infarcts account for 5.5 million deaths worldwide each year and are a leading cause of long-term disability (1–3). Despite tremendous progress in our understanding of the pathophysiology of strokes, ongoing efforts to identify novel molecular targets have yet to yield new therapies. Recombinant tissue plasminogen activator remains the only medication specifically approved by national regulatory agencies for use in patients with ischemic stroke; however, for a variety of reasons, it is used in less than 20% of stroke victims (4–7). Moreover, its use is associated with an increased risk of intracranial hemorrhage (8). Despite the devastating effects of malignant cerebral edema on large territorial infarcts, the only pharmacotherapeutic option for this complication is osmotherapy, the effects of which remain unproven. There remains a critical need to improve our understanding of the molecular pathogenesis of this devastating neurologic condition to identify more effective therapeutic strategies.

Transient receptor potential melastatin 4 (Trpm4) is a member of a large protein superfamily consisting of 28 mammalian cation channels (9,10). Most members of the Trp family are permeable to divalent cations. The exceptions—Trpm4 and Trpm5—are Ca²⁺-impermeable channels that transport monovalent cations exclusively and nonselectively (9,10). Transient receptor potential melastatin 4 channels are activated by an increase in cytosolic Ca²⁺ or by a decrease in cytosolic ATP (11). Accumulating data show that there is upregulation of Trpm4 in microvascular endothelial cells, neurons, and glia in experimental rat models of stroke, spinal cord injury, and subarachnoid hemorrhage (12–15). Emerging evidence suggests that Trpm4 interacts with sulfonylurea receptor 1 (Sur1) to form a novel ion channel, the Sur1-Trpm4 channel (15), which functions critically in the pathophysiology of various acute CNS injuries. Sulfonylurea receptor 1-Trpm4 channels contribute to cytotoxic edema, serve as end-executioners in accidental necrotic death induced by ATP depletion or reactive oxygen species (16), and participate in blood-brain barrier breakdown and formation of ionic and vasogenic edema (14,17).

Expression of Trpm4 has been investigated in tissue specimens obtained from patients with multiple sclerosis (18) and subarachnoid hemorrhage (14), but it has not yet been studied in human cerebral infarcts. Here, we sought to determine whether upregulation of Trpm4 protein and messenger

RNA (mRNA) is present in infarcted human cerebral cortex and whether Trpm4 protein coassociates with Sur1 to form Sur1-Trpm4 channels in focal cerebral ischemia in humans, and we tested the effects of a selective inhibitor of sulfonyleurea receptor on an animal model of acute cerebral ischemia.

MATERIALS AND METHODS

Human Tissues

The tissue collection protocol was approved by the Institutional Review Board of the University of Maryland (Baltimore, MD). Patients who died within 31 days of cerebral ischemia documented between January 2010 and December 2012 and who underwent autopsy were identified retrospectively by reviewing the records of the Department of Pathology at the University of Maryland School of Medicine. Within these constraints, 15 focal cerebral infarcts originating from 13 patients were identified. For comparison, contralateral cortex samples were evaluated as control tissue. Brain specimens from 6 patients with documented absence of ischemic lesions also were examined as controls. For additional validation of antibodies, sections of normal colon surgically removed from 2 patients during bypass surgery were also evaluated. Standard tissue fixation protocols (7–10 days in formalin) were applied.

Histologic validation of the presence or absence of an ischemic lesion in brain specimens was performed by a neuropathologist in all cases. Representative paraffin-embedded tissue blocks were selected from each case for detailed evaluation. For normal brains, blocks encompassing representative frontal or parietal cortices were studied. Blocks were sectioned at 6 μ m and stained with hematoxylin and eosin or prepared for immunohistochemistry.

Rat Model of Middle Cerebral Artery Occlusion

Animal experiments were performed following a protocol approved by the Institutional Animal Care and Use Committee of the University of Maryland. All experiments were performed in accordance with relevant guidelines and regulations in the US National Institutes of Health Guide for the Care and Use of Laboratory Animals. All efforts were made to minimize the number of animals used and their suffering.

Male Wistar rats (275–325 g; Harlan, Indianapolis, IN) were anesthetized (ketamine 60 mg/kg and xylazine 7.5 mg/kg intraperitoneally). Peripheral capillary oxygen saturation (SpO₂) via pulse oximetry and temperature were carefully regulated, and all surgical procedures were performed aseptically. Middle cerebral artery occlusion (MCAo) was achieved using an intraluminal thread. A midline incision was made to expose the right common carotid artery, external carotid artery, and internal carotid artery. A 4-0 monofilament nylon suture with a rounded tip approximately 0.26 mm in diameter was inserted via the external carotid artery into the internal carotid artery and was advanced by approximately 18 mm to occlude the middle cerebral artery, as monitored by Doppler flowmetry. After 120 minutes, the occluder was removed to allow reperfusion. The external carotid artery stump was ligated, and the neck incision was closed. Using an automatic homeothermic blanket control unit, we maintained animal body temperature at 37°C throughout the procedure and during postsurgical

recovery. After the procedure, 12 rats were randomly assigned to vehicle treatment (n = 6) or glibenclamide treatment (n = 6). At 48 hours, the animals were killed and their brains were analyzed for tumor necrosis factor (TNF) expression.

Glibenclamide Treatment

Drug formulation of glibenclamide (number G2539; Sigma, St Louis, MO) in dimethyl sulfoxide and preparation of miniosmotic pumps were performed as previously described (19). Treatment consisted of intraperitoneal administration of a single loading dose of glibenclamide (10 μ g/kg) or an equivalent volume of vehicle within 10 minutes of ischemia and continuous infusion (1.0 μ L/hour) via miniosmotic pumps (Alzet 2001; Alzet Corp, Cupertino, CA) beginning at the end of surgery, resulting in delivery of 200 ng/hour or an equivalent volume of vehicle subcutaneously for 1 week. The dose of glibenclamide used does not result in hypoglycemia (17).

Antibodies

The custom anti-Trpm4 and anti-Sur1 antibodies used have been previously described (15). The antigenic peptide for Trpm4 was the N-terminal intracellular domain of mouse Trpm4, corresponding to amino acids 1 to 612 (NP 780339). Anti-Trpm4 antibodies were raised in chicken and used at 1:200 dilution. The antigenic peptide for Sur1 was the intracellular nucleotide-binding domain 1 of Sur1 (rat Sur1 complementary DNA amino acids 598–965 of NP 037171). Anti-Sur1 antibodies were raised in rabbit and used at 1:200 dilution. Other primary antibodies included the following: rabbit anti-cytokeratin 20 (prediluted; Ventana, Tucson, AZ) for colonic epithelial cells; mouse anti-gial fibrillary acidic protein (GFAP) (1:500, CY3-conjugated, C-9205; Sigma) for astrocytes; mouse anti-NeuN (1:100, MAB377; Chemicon, Temecula, CA) for neurons; goat anti-CD31 (PECAM-1) (1:200, sc-1506; Santa Cruz Biotechnology, Santa Cruz, CA) for endothelial cells; goat anti-immunoglobulin G (IgG) (1:500, fluorescein isothiocyanate [FITC]-conjugated, NB7477; Novus Biologicals, Littleton, CO) for IgG; goat anti-TNF (1:100, sc-1350; Santa Cruz Biotechnology) for TNF; rabbit anti-myeloperoxidase (1:200, A0398; Dako, Carpinteria, CA) for neutrophils; and mouse anti-rat endothelial cell antigen 1 (1:100, MA1-81510; Thermo Fisher, Rockford, IL) for rat endothelium.

Immunohistochemistry and Förster Resonance Energy Transfer

Deparaffinized sections were rinsed in ethanol and washed with phosphate-buffered saline (PBS; 10 mmol/L, pH 7.4). For antigen retrieval, slides were placed in citrate buffer (10 mmol/L, pH 8.0), heated in a microwave oven at 900 W for 10 minutes, and washed in PBS. Slides were incubated with a mixture of 5% goat serum (Sigma) and 0.2% Triton X-100 for 1 hour at room temperature before overnight incubation at 4°C with anti-Trpm4 and/or anti-Sur1 antibodies and, in some cases, with a cell-specific or anti-IgG primary antibody. Slides were rinsed again in PBS. Single-label immunohistochemistry for Trpm4 was developed using biotin-conjugated secondary antibody. Sections were incubated in PBS with 0.3% H₂O₂ for 30 minutes to block endogenous peroxidase activity. After overnight incubation with primary

antibody, sections were incubated with biotinylated secondary antibody (1:500, BA-1000, goat anti-chicken; Vector Laboratories, Burlingame, CA) for 2 hours. After washing in PBS, sections were incubated in avidin biotin solution (Vector Laboratories), and color was developed in diaminobenzidine chromogen solution (0.02% diaminobenzidine in sodium acetate 0.175 mol/L) activated with 0.01% hydrogen peroxide. Cresyl violet was used as counterstain to visualize cell nuclei. Sections were rinsed, mounted, dehydrated, and coverslipped with DPX mounting medium (Electron Microscopy Services, Fort Washington, PA). Omission of primary antibodies was used as negative control.

To show localization of Trpm4 and/or Sur1 within identified cell types and/or coexpression with IgG, we performed immunofluorescence microscopy of anti-Trpm4 or anti-Sur1 antibodies in addition to cell-specific and anti-IgG primary antibodies using the standard protocol, as described previously. Slides were incubated for 1 hour with fluorescence-labeled species-appropriate secondary antibodies (1:500, Alexa Fluor 488 and Alexa Fluor 555; Invitrogen/Molecular Probes, Eugene, OR) at room temperature. Omission of primary antibody was used as negative control. Sections were coverslipped with polar mounting medium containing anti-fade reagent and 4',6-diamidino-2-phenylindole (DAPI; Invitrogen). Immunolabeled sections were visualized using epifluorescence microscopy (Nikon Eclipse 90i; Nikon Instruments Inc, Melville, NY).

Antibody-based Förster resonance energy transfer (FRET) was performed on acute lesions (Cases 1–4) using anti-Sur1 and anti-Trpm4 antibodies, as described (14,15), except that FRET imaging and measurements of FRET efficiency were performed using a Zeiss LSM710 confocal microscope.

Analysis of Trpm4, Sur1, IgG, and TNF Protein Expression

Transient receptor potential melastatin 4 immunoreactivity was analyzed for each cell type–specific marker for each case (Table). All sections were immunolabeled as a single batch, and all images were collected using uniform parameters of magnification and exposure, as previously described (20,21). Two areas encompassing ischemic lesions or controls were randomly selected for construction of a montage, with each montage composed of 16 images (each 300 × 400 μm) acquired at 20× magnification. Images were independently evaluated by 2 observers who were blinded to demographic and clinical data. Specific Trpm4 immunoreactivity associated with each cell type–specific marker for each case was evaluated. Areas of maximal labeling were scored for each case using a semiquantitative scale ranging from 0 to 4 as follows: 0, none; 1 (+), weak punctuate labeling present in rare cells (<10%); 2 (++) , weak punctate staining in scattered cells or aggregates (<50%); 3 (+++) strong punctate staining present in many cells (>50%); 4 (++++) strong diffuse staining of most cells (>90%). The overall concordance between the 2 observers was more than 90%. In cases of disagreement, independent re-evaluation was performed by both observers to arrive at the final score. Sulfonylurea receptor 1 immunoreactivity for each cell type–specific marker for each case had been previously reported (22).

Unbiased measurements of specific IgG or TNF labeling within regions of interest were obtained, using NIS-Elements AR software (Nikon Instruments), from sections of acute lesions (Cases 1–4) and controls immunolabeled in a single batch, as previously described (23). All region-of-interest images for a given signal were captured using uniform parameters of magnification, area, exposure, and gain. To quantify IgG or TNF, we defined a circular region of interest as a perimeter encompassing vessels (with a diameter twice that of the vessels) within the infarct or control brain. For each region of interest, a histogram of pixel intensity was constructed to determine the intensity of background labeling. Pixels within the region of interest were defined as having specific labeling if their intensity was more than 3 times that of background. The area occupied by pixels with specific labeling was used to calculate the percentage of the region of interest with specific labeling.

In Situ Hybridization of Trpm4 mRNA

Digoxigenin (DIG)–labeled probes (antisense, 5'-CCGAGAGTGGGAATCCCGGATGAGGCGGTAACGCTGC-3'; sense, 5'-GCAGCGTTACCGCCTCATCCGGGAATCCACTCTCGG-3'), designed to hybridize nucleotides 3288 to 3324 located within the coding sequence of the human *Trpm4* gene (NM 017636), were supplied by Integrated DNA Technologies Inc (Coralville, IA). In situ hybridization was performed on 10-μm-thick sections of acute lesions (Cases 1–4) and controls using an IsHyb In Situ Hybridization Kit (Biochain Institute Inc, Newark, CA), according to the manufacturer's protocol. Deparaffinization and rehydration were performed as described previously. Sections were incubated in diethyl pyrocarbonate (DEPC)–treated PBS and fixed in 4% paraformaldehyde in PBS for 20 minutes. After being rinsed twice with DEPC-PBS, slides were treated with proteinase K 10 μg/mL at 37°C for 10 minutes. Slides were washed in DEPC-PBS, rinsed with DEPC-H₂O, and prehybridized with ready-to-use prehybridization solution (BioChain Institute Inc) for 3 hours at 50°C. The DIG-labeled probe was diluted in hybridization buffer (BioChain Institute Inc) and applied at 4 ng/μL. Sections were incubated at 45°C for 16 hours. Posthybridization washing and immunologic detection, using anti-DIG alkaline phosphatase with nitro blue tetrazolium/5-bromo-4-chloro-3-indolyl-phosphate as substrate, were performed as recommended by the manufacturer. Alkaline phosphatase–conjugated anti-DIG antibodies (1:100, PBS-diluted; BioChain Institute Inc) were incubated on slides for 2 hours. Finally, slides were rinsed in distilled H₂O and immunolabeled for Trpm4 protein using a fluorescent secondary antibody, as described previously. The dark-purple reaction product represents *Trpm4* mRNA; green fluorescence indicates immunohistochemical staining for Trpm4 protein. In situ hybridization of Sur1 has been previously reported (22).

Statistical Analysis

Two-tailed Fisher exact test was used to determine the contingency of absent or weak (0/+ /++) versus prominent or diffuse (+++/++++) Trpm4 staining in different cell types present within infarcted and noninfarcted cortices. Scores for Trpm4 expression in different cell types were additionally

TABLE. Trpm4 Protein Expression in Brain Tissue Samples

Case No.	Capillaries	Venules	Arterioles	Neurons	Astrocytes	Neutrophils	Postinfarct Interval (days)
Focal ischemic infarcts							
1	+++	++	+++	++++	++	+++	1
2	++	++	+++	+++	++	+++	3
3	++++	++	+++	+++	++	+++	5
4	++	++	++	+++	++	++++	5
5	++++	+++	++++	+++	++	++++	7
6	++++	+++	++++	+++	++	++++	7
7a	+++	++	+++	+++	++	+++	7
7b	+++	++	+++	+++	++	++++	7
8	++	+++	++	+++	++	+++	15
9	++++	++++	++++	++	+++	++++	15
10	++	+++	++++	+++	++++	++++	16
11	++	+++	++++	++	++++	++++	26
12	+++	++++	++++	++	++++	+++	30
13a	+++	++	+++	++	+++	+++	31
13b	++	++	++	++	++++	++++	31
Contralateral							
1	+	0	+	+	++	0	1
2	0	0	0	+	++	+	3
3	+	0	+	+	++	0	5
4	0	0	+	0	+	0	5
5	+	0	+	+	++	+	7
6	0	0	0	0	0	+	7
7a	0	0	+	+	++	++	7
7b	+	0	+	++	0	+	7
8	+	0	0	++	++	0	15
9	0	0	0	0	+	+	15
10	+	0	+	+	++	0	16
11	0	0	+	+	+	+	26
12	0	+	+	0	+	++	30
13a	0	0	++	+	++	+	31
13b	0	0	+	+	++	+	31
Control brains							
14	0	0	0	0	0	0	N/A
15	0	0	0	0	0	+	N/A
16	+	0	0	+	+	0	N/A
17	0	0	0	0	0	0	N/A
18	0	0	+	0	+	+	N/A
19	+	0	+	+	+	0	N/A

Semiquantitative scores are as follows: 0, none; (+) weak punctuate labeling present in rare cells (<10%); (++) weak punctuate staining in scattered cells or aggregates (<50%); (+++) strong punctuate staining in many cells (>50%); (++++) strong diffuse staining in most cells (>90%).

N/A, not applicable.

analyzed as a function of postmortem and postinfarct intervals by calculating Spearman correlation coefficient. Both IgG labeling and TNF labeling were analyzed using Student *t*-test. Calculations were performed using OriginPro version 8 (Origin Lab Corp, Northampton, MA).

RESULTS

Positive and Negative Controls

The custom anti-Trpm4 antibody used here had been validated previously in rat and human cerebral tissues (14,15). The specificity of the antibody batch used for this study was further validated in human colon epithelium, which is known

to express high levels of Trpm4 (Fig. 1) (24). Omission of primary antibody and tissues obtained from Trpm4 knockout mice were used as negative controls and confirmed the specificity of labeling (data not shown).

Trpm4 Expression in Infarcted Cerebral Cortex

Ischemic lesions originated from 15 men and 5 women, with age at death ranging from 32 to 84 years (mean, 61 years) (Table). Normal specimens originated from 4 men and 2 women who had died rapidly of nonneurologic diseases (i.e. acute cardiovascular or respiratory disorders). Postmortem interval ranged between 12 and 80 hours. Additional demographic data on these patients have been reported (22).

Transient receptor potential melastatin 4 protein expression in infarcted and noninfarcted cortices was analyzed using immunohistochemistry. Representative sections of acute infarcts are shown in Figure 2. Immunoperoxidase preparations revealed prominent Trpm4 immunoreactivity in virtually all neural and vascular cells (Table; Fig. 2A), whereas noninfarcted contralateral and control cortices demonstrated only weak immunoreactivity in rare cells and/or background neuropil (Table; Fig. 2B).

Immunofluorescent preparations further demonstrated marked upregulation of Trpm4 in neural and vascular cells in ischemic infarcts (Figs. 2C, E, G, I, K). Endothelial cells of capillaries, arterioles, and venules exhibited diffuse membranous and cytoplasmic expression and colabeled for the endothelial cell marker PECAM-1 (CD31) (Figs. 2C, E, G).

Transient receptor potential melastatin 4 immunolabeling also was prominent in neurons immunoreactive to NeuN (Fig. 2I) and in astrocytes immunoreactive to GFAP (Fig. 2K). Neurons, endothelial cells, and astrocytes in noninfarcted contralateral and control cortices exhibited weak or no Trpm4 labeling (Table; Figs. 2D, F, H, J, L).

In situ hybridization studies showed de novo transcriptional upregulation of *Trpm4* mRNA in acute lesions. We observed strong labeling of cortical endothelial cells of capillaries, arterioles, and venules, and upregulation in neurons (Fig. 3, middle column) within ischemic cortices. In situ hybridization signals for *Trpm4* mRNA were present in cells that were strongly immunopositive for Trpm4 protein (Fig. 3, left column), whereas contralateral and control cortices showed only faint in situ labeling in rare cells (Fig. 3, right column).

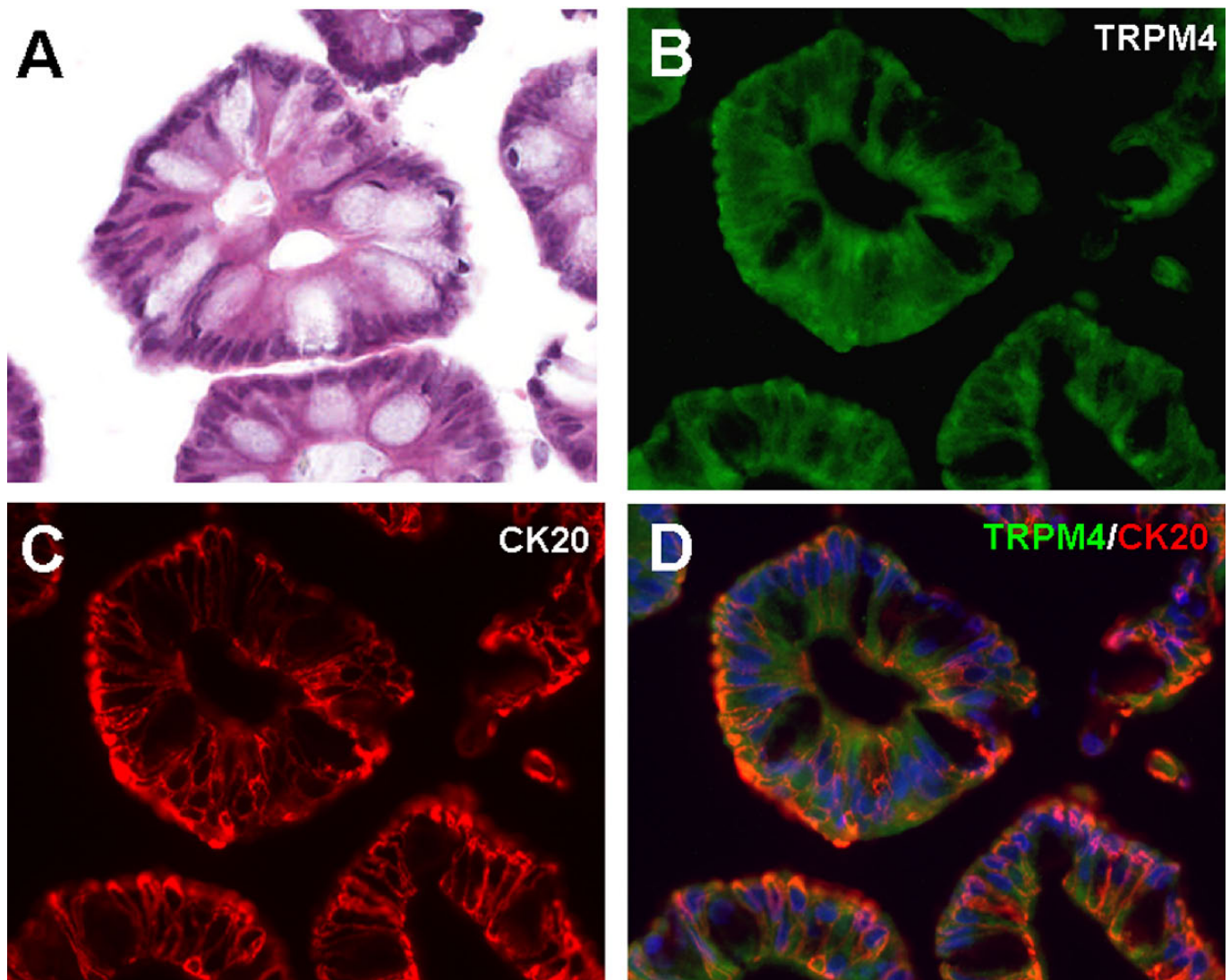
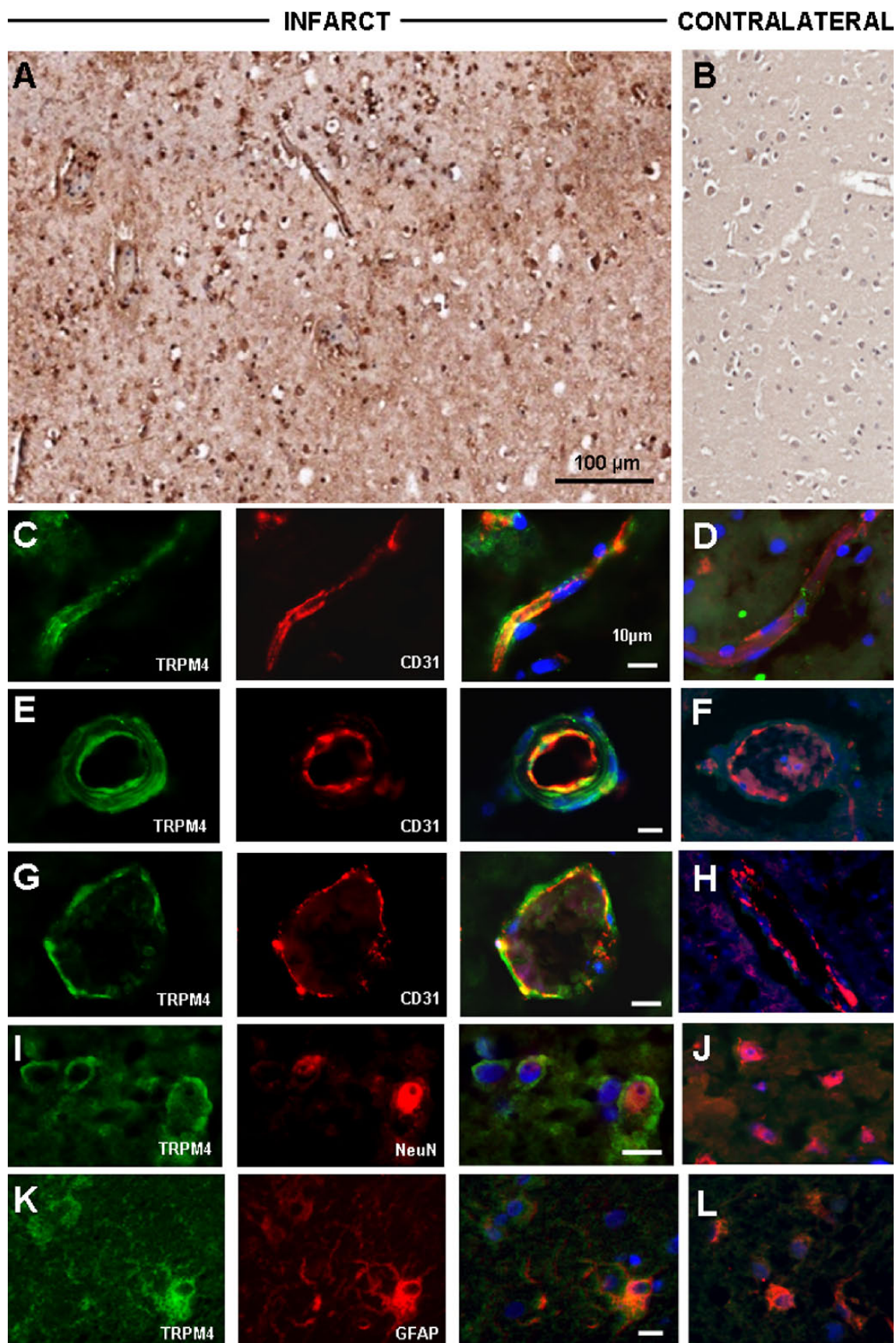


FIGURE 1. Positive controls for Trpm4 immunohistochemistry. **(A)** Hematoxylin and eosin–stained section of normal colon shows villus epithelial cells. Immunohistochemistry with primary antibodies against Trpm4 protein shows cytoplasmic labeling of colonic epithelial cells **(B)** and colocalization with cytokeratin 20 (CK20) **(C)**. Merged fluorescent image is shown in **(D)**. Scale bar = 50 μ m. Green/FITC, Trpm4; red/CY3, CK20; blue/DAPI.



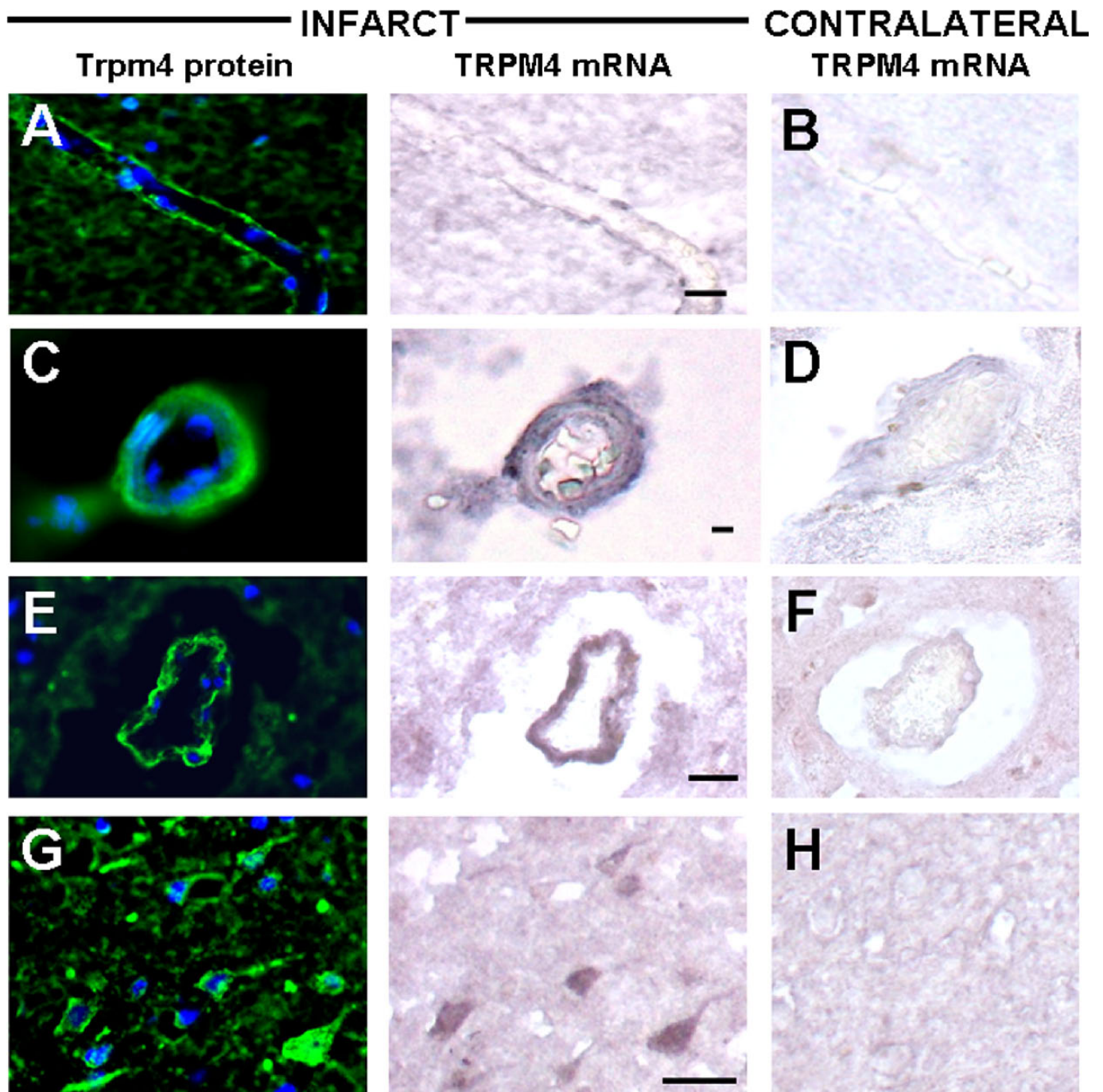


FIGURE 3. In situ hybridization shows upregulated *Trpm4* mRNA in acute ischemic infarcts. Tissues from recently infarcted cortex are hybridized with antisense probe and labeled with immunohistochemical stain directed against Trpm4 protein; dual labeling for *Trpm4* mRNA and Trpm4 protein is identified within endothelial cells in capillaries (**A**), arterioles (**C**), and venules (**E**), and in scattered neurons (**G**) in ischemic tissues (**A, C, E, G**) versus contralateral cortex (**B, D, F, H**). Original magnification: 20 \times . Scale bar = 10 μ m. Images shown are from Cases 3 and 6.

FIGURE 2. Protein Trpm4 is upregulated in focal cerebral infarcts. Low-power images of immunohistochemistry with diaminobenzidine chromogen staining showing upregulation of Trpm4 in neural and vascular cells of infarcted cortex (**A**) in comparison with control (**B**). With fluorescent double labeling, increased Trpm4 protein is observed within CD31-positive capillaries (**C**), arterioles (**E**), and venules (**G**), and within NeuN-positive neurons (**I**) and GFAP-positive astrocytes (**K**) in ischemic tissues (**C, E, G, I, K**) versus contralateral control tissue samples (**D, F, H, J, L**). Merged images of double labeling are shown in the third and fourth columns. Original magnification: 20 \times (**A, B**) or 40 \times (**C–N**). Scale bars = (**A**) 100 μ m; (**C, E, G, I, K, M**) 10 μ m. Green/FITC, Trpm4; red/CY3, PECAM-1 (CD31), NeuN, or GFAP; blue/DAPI. Images shown are from Cases 3 and 6.

Time Course of Trpm4 Expression in Ischemic Cells

Transient receptor potential melastatin 4 expression in different cell types was evaluated semiquantitatively at various times after the onset of ischemic events. There were no

significant differences in any cell type as a function of post-mortem interval, but upregulated protein was found in neural and vascular cells as early as 1 day after the clinical onset of ischemia; it remained elevated in specimens obtained from patients who died up to 30 days after the clinical onset of

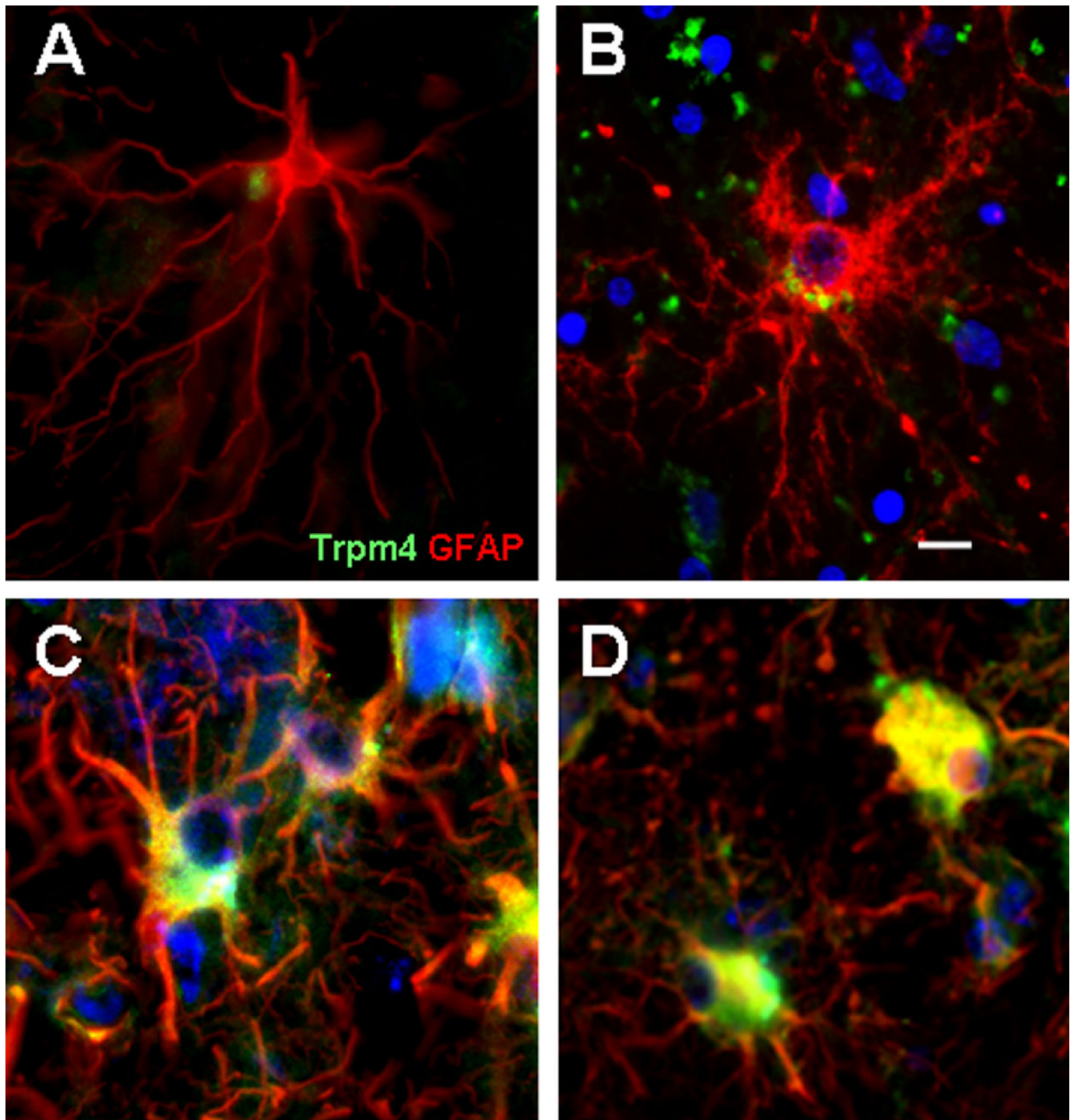


FIGURE 4. Unique pattern of Trpm4 immunoreactivity in astrocytes. Astrocytes show perinuclear dot-like immunoreactivity for Trpm4 in normal cortex (**A**), with prominent perinuclear accentuation in acute infarcts (**B**) and intensified cytoplasmic and distal process staining in subacute infarcts (**C**, **D**). Original magnification: 20 \times . Scale bar = 10 μ m. Green/FITC, Trpm4; red/CY3, GFAP; nuclei stained with DAPI. Merged images shown are from Cases 19, 1, 9, and 13b.

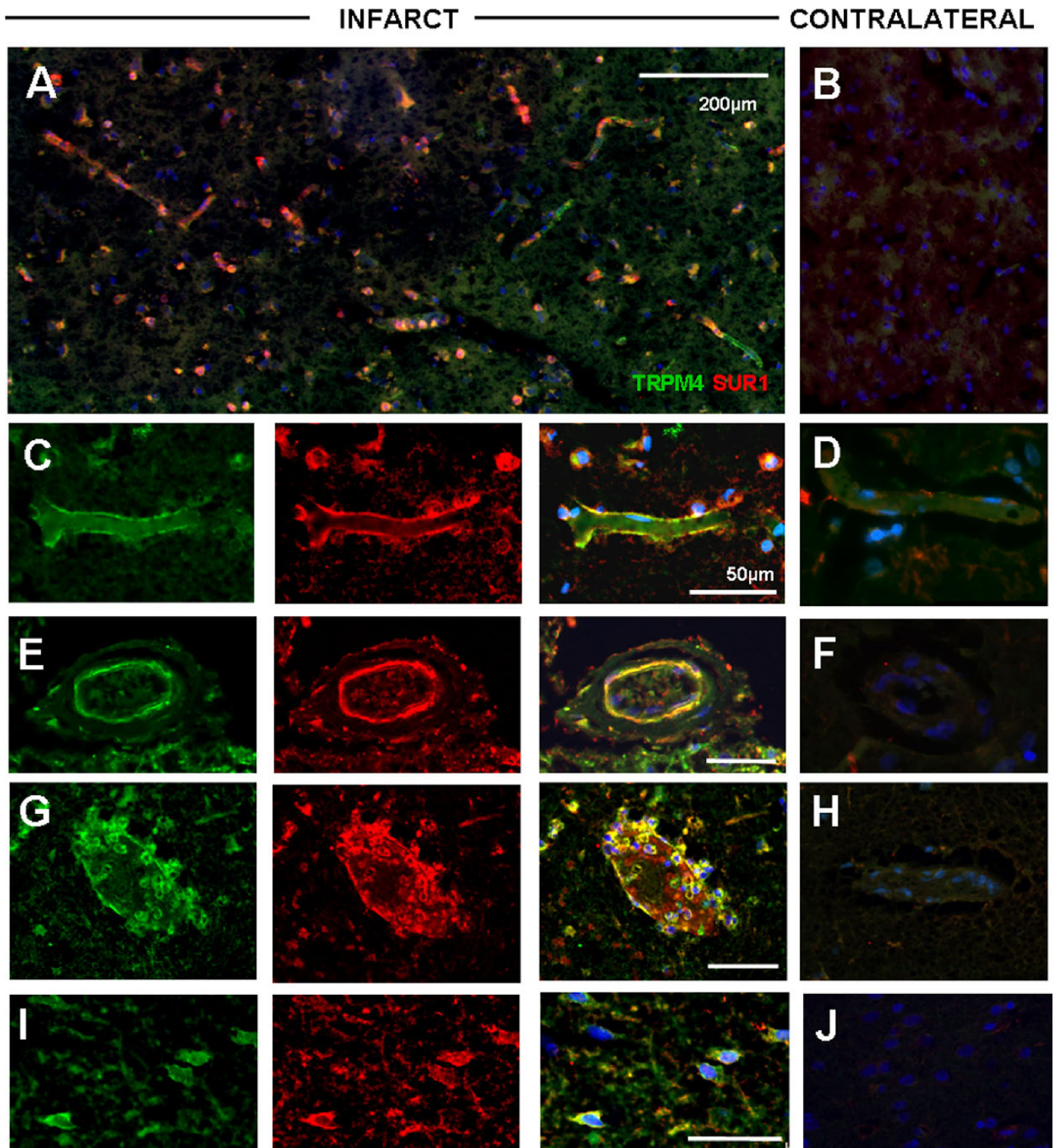
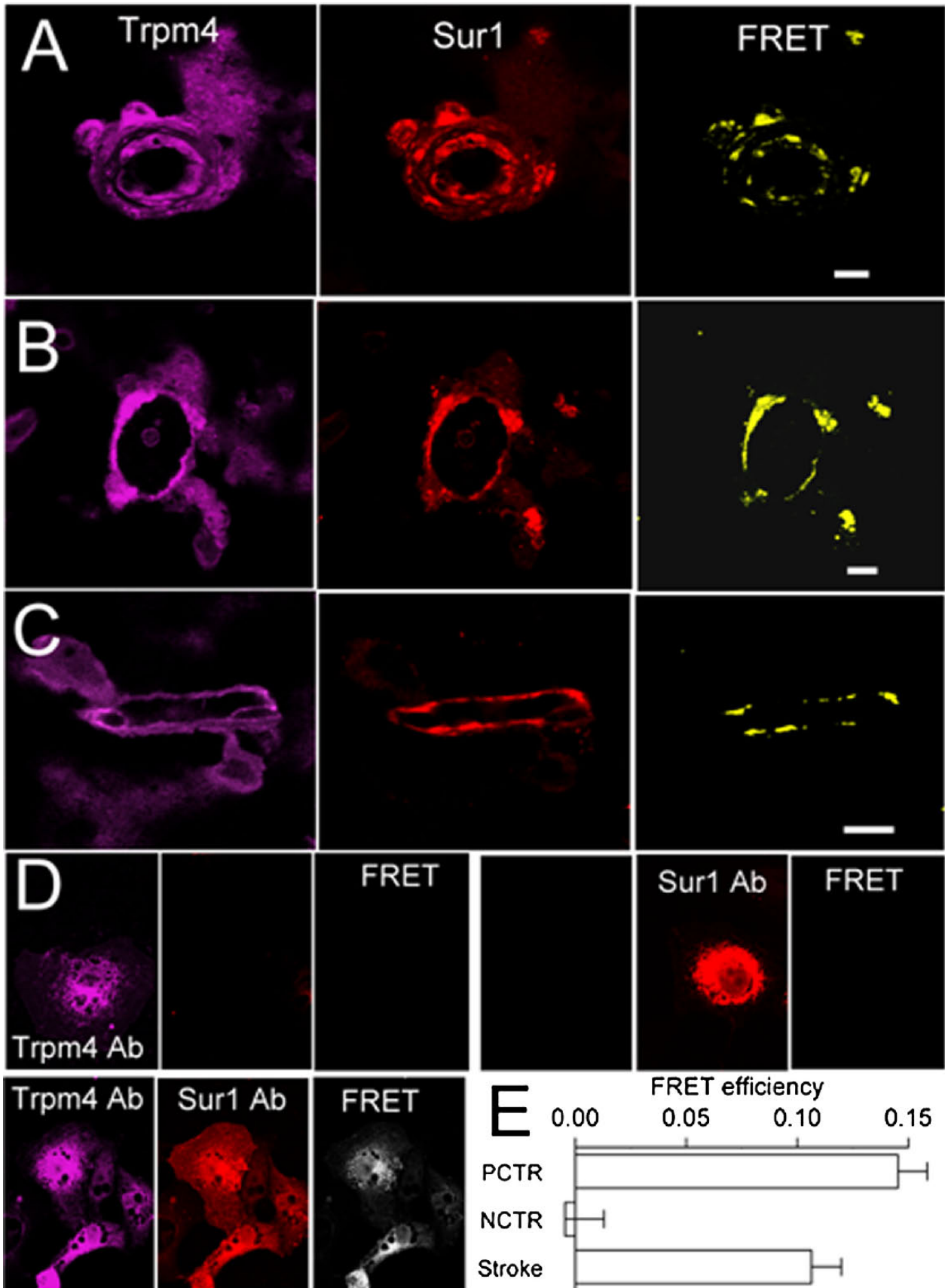


FIGURE 5. Proteins Trpm4 and Sur1 are upregulated and colocalized in acute ischemic infarcts. Fluorescent double-labeling studies demonstrate prominent expression in scattered neural and vascular cells of an acute infarct (**A**) relative to contralateral brain (**B**). High-power images of infarcted cortex show colocalization of proteins within capillaries (**C**), arterioles (**E**), venules and neutrophils (**G**), and within neurons (**I**) present within infarcted cortex. There is negligible staining in controls (**D**, **F**, **H**, **J**). Original magnification: 20 \times . Scale bar = 10 μ m. Green/FITC, Trpm4; red/CY3, Sur1; blue, DAPI. Images shown are from Cases 2 and 3.



stroke. Significant differences in staining intensities were found in all cell types, relative to controls ($p < 0.05$ for astrocytes; $p < 0.01$ for endothelial cells, neurons, and neutrophils) (Table). Neurons stained prominently in acute lesions, with mild regression of staining noted with postinfarct interval ($p < 0.01$) (Table). Endothelial cells and neutrophils exhibited sustained Trpm4 upregulation across time (Table). Astrocytes exhibited a unique pattern of Trpm4 immunoreactivity: In noninfarcted cortex, Trpm4 appeared as punctate perinuclear staining, whereas a progressive increase in the extent of cytoplasmic and membranous immunopositivity was observed with postinfarct interval ($p < 0.01$) (Table; Fig. 4).

Trpm4 and Sur1 Proteins Are Coexpressed and Coassociated

Sulfonylurea receptor 1 was previously reported to be upregulated in endothelial cells, neurons, and astrocytes in infarcted cerebral cortices (22). Here, we found that upregulated Trpm4 colocalized with Sur1 in endothelial cells, neurons, and astrocytes in infarcted cerebral cortices (Fig. 5). We used FRET to determine whether colocalized proteins also coassociated. Förster resonance energy transfer analysis demonstrated that Sur1 and Trpm4 coassociated in endothelial cells (Figs. 6A–D) and neurons. Förster resonance energy transfer efficiency, which reflects the proximity of 2 fluorophores, was 13% in infarcted cortices and 0% in controls (Fig. 6E).

Pathologic Correlates of Sur1-Trpm4 Channel Upregulation in Cerebral Infarcts

Sulfonylurea receptor 1–positive/Trpm4–positive endothelial cells and Sur1–positive/Trpm4–positive neurons present in infarcted cerebral cortex and peri-infarct zones showed prominent membrane irregularities and frank blebbing, consistent with cytotoxic edema (Fig. 7A). Coexpression of Sur1 and Trpm4 in abnormal-appearing endothelial cells also was associated with vasogenic edema, as evidenced by upregulated perivascular labeling for IgG (Figs. 7B–G), TNF (Fig. 7I), and myeloperoxidase (Fig. 7J). Membrane blebbing was not identified in Trpm4–negative neural or vascular cells. In addition, membrane blebbing was not seen in Trpm4–negative or Trpm4–positive astrocytes present in infarcted or noninfarcted cortices (Fig. 4).

Inhibition of Sur1 in a Rat Model of MCAo Stroke

To assess the consequences of Sur1-Trpm4 channel expression, we evaluated the effects of pharmacologic inhibition of Sur1 with glibenclamide in a rat model of MCAo stroke. Extravasation of serum proteins is known to promote neuroinflammation. Inhibition of Sur1 was found to mitigate

expression of TNF, an acute-phase reactant cytokine (Fig. 8), suggesting a critical proinflammatory role for Sur1-Trpm4 channel expression in focal cerebral ischemia.

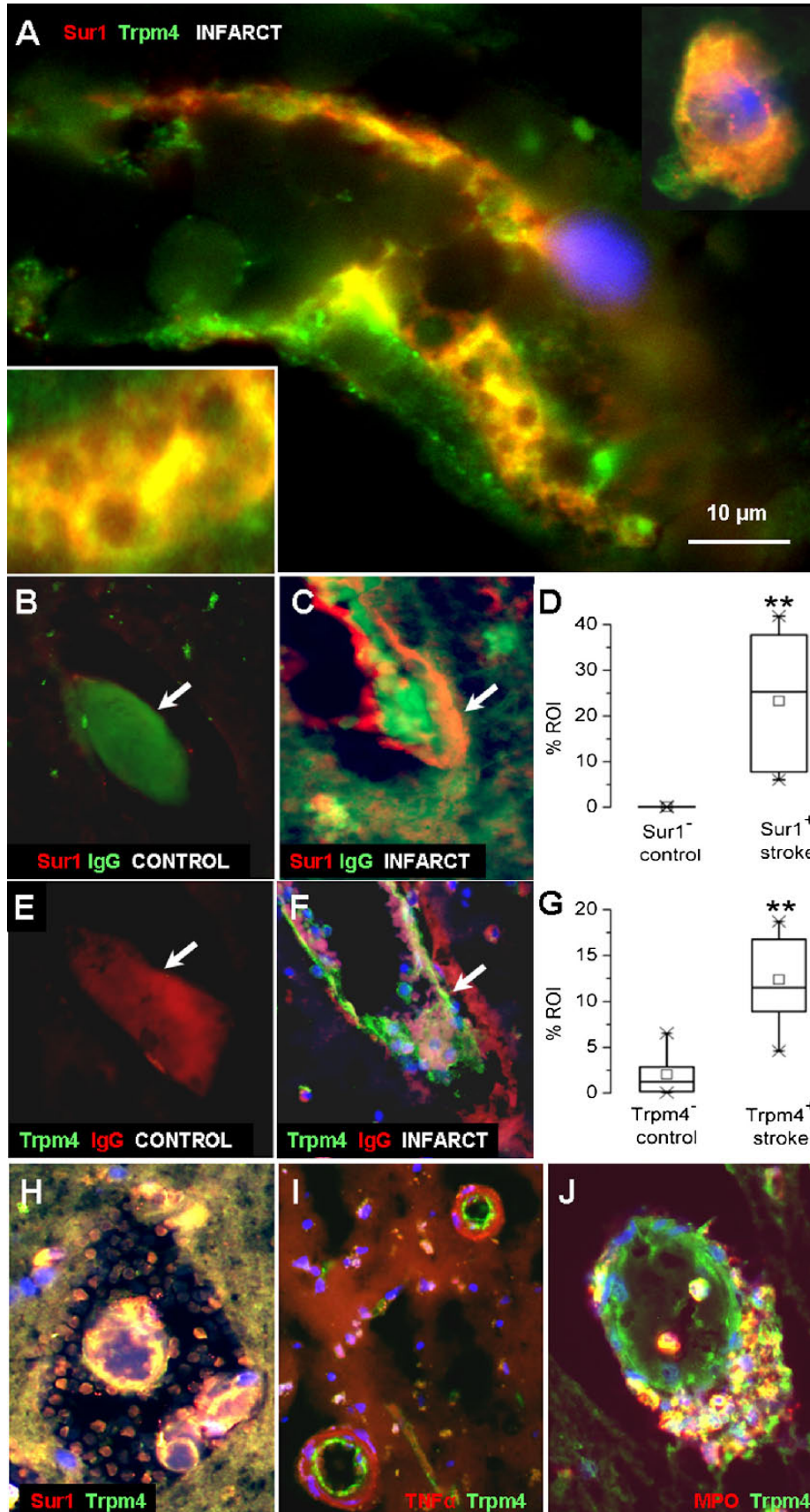
DISCUSSION

This is the first report to systematically analyze Trpm4 expression in adult human brains after the onset of focal cerebral ischemia. Our findings indicate that *Trpm4* mRNA and Trpm4 protein are upregulated in infarcted human cortex. The current study is in accordance with a report of Trpm4 upregulation in a preclinical model of stroke (13). In contrast to the findings in the animal model, however, our study showed that Trpm4 upregulation was sustained in infarcted human tissues during acute and subacute postischemic intervals. Analysis of Trpm4 expression in human neurologic disease was previously limited to specimens originating from patients with multiple sclerosis (18) or subarachnoid hemorrhage (14). Significant upregulation of Trpm4 was identified under both neuropathologic conditions. In animal models, Trpm4 expression has been associated with inflammation-induced axonal and neuronal injuries in demyelinating lesions (18). Furthermore, endothelial cell upregulation of Trpm4 has been associated with inflammation and blood-brain barrier permeability in a model of subarachnoid hemorrhage (14), and with capillary fragmentation and secondary hemorrhage in a model of spinal cord injury (12). Together, these studies suggest a critical function for Trpm4 in acute CNS injuries of varying etiology.

In a prior analysis, we showed prominent upregulation of Sur1 (a member of the ATP-binding cassette protein superfamily) in neural and vascular cells of these same post-mortem infarct specimens (22). The current study complements our prior findings and is the first to report that Trpm4, a voltage-dependent cation channel, colocalizes with Sur1 in neurons, endothelial cells, astrocytes, and neutrophils present in human cerebral infarcts. Furthermore, this is the first study to document, via antibody-based FRET, the coassociation of upregulated Trpm4 and Sur1 in human cerebral infarcts. Together, the findings indicate that Sur1-Trpm4 channels (formerly known as Sur1-regulated NC_{Ca-ATP} channels) are present in infarcted human cerebral cortex, but not in non-infarcted control specimens.

The Sur1-Trpm4 cation channel is not constitutively present in CNS tissues but is transcriptionally upregulated de novo under neuropathologic conditions. Recent data showed stable heteromultimeric assembly of Sur1 and Trpm4 and demonstrated that Sur1 regulates the calcium sensitivity of Trpm4, the pore-forming subunit of the Sur1-Trpm4 channel

FIGURE 6. Proteins Trpm4 and Sur1 coassociate in acute ischemic infarcts. Immunolabeled sections reveal coexpression of Trpm4 and Sur1, with FRET signals elicited in cortical arterioles (A), venules (B), and capillaries (C) in ischemic infarcts. (D) Validation of antibodies (Abs) for Ab-based FRET analysis. COS-7 cells expressing either Trpm4 or Sur1 (top) or coexpressing both (bottom) were incubated with either anti-Sur1 or anti-Trpm4 Abs (top) or both (bottom), followed by anti-rabbit Cy3-conjugated plus anti-goat Cy5-conjugated secondary Abs. Fluorescence images of the 2 fluorophores (left and middle columns) and FRET images (right column) are shown. Data are representative of 6 replicates. Note that the primary Abs against Sur1 and Trpm4 do not cross-react. (E) Förster resonance energy transfer efficiencies in positive controls (PCTR), negative controls (NCTR), and infarcts (Stroke). Scale bar = 10 μ m.



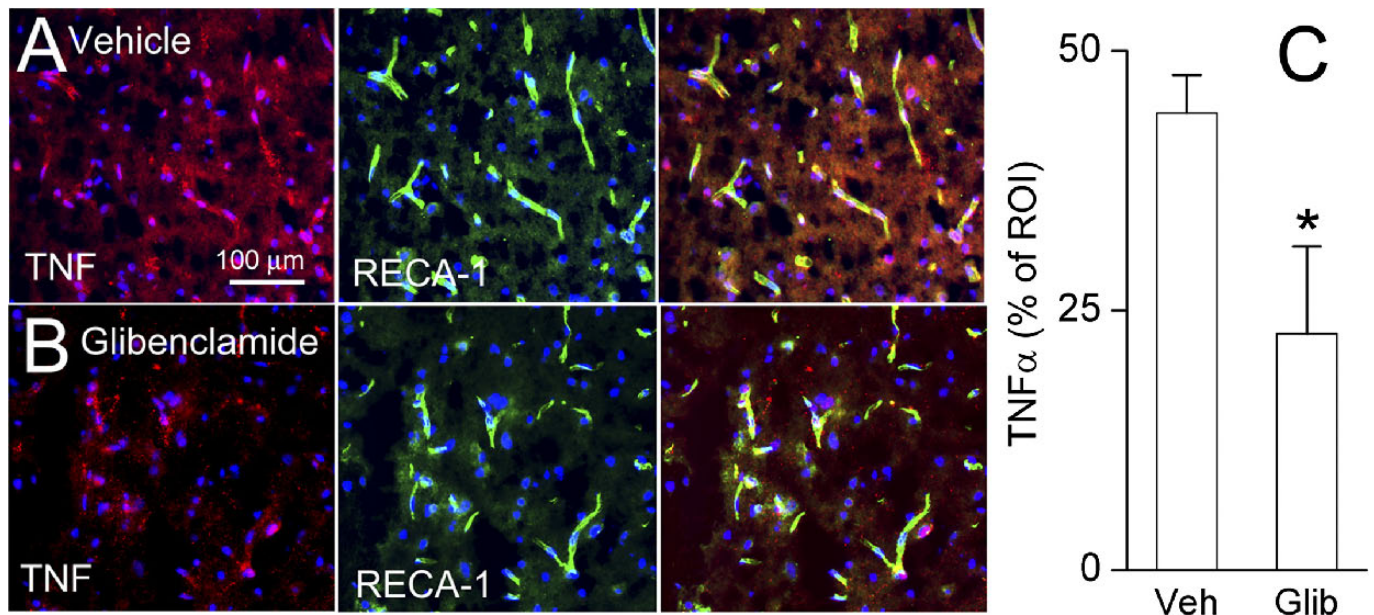


FIGURE 8. Pharmacologic inhibition of the Sur1-Trpm4 channel in a rat model of MCAo stroke mitigates TNF expression. Penumbra cortex immunolabeled for TNF (left; red) and rat endothelial cell antigen 1 (RECA-1; middle; green) in rats treated with vehicle (Veh) (A) or glibenclamide (Glib) (B). Merged images are shown to the right. Bar graph of quantitative regions of interest (ROI) analysis is shown (C). * $p < 0.05$ (6 rats per group).

(15). The channel is activated by a rise in intracellular Ca^{2+} or by depletion of intracellular ATP. Channel activation induces monovalent cation influx that results in cell membrane depolarization.

Ca^{2+} is an important second messenger, and significant amounts of energy are expended to maintain intracellular concentrations of free Ca^{2+} at physiologic levels (~10,000-fold lower than extracellular levels). Because a large electrochemical driving force promotes Ca^{2+} influx into cells, homeostasis requires Ca^{2+} extrusion, which is achieved through the plasma membrane Ca^{2+} -ATPase pump, the Na^+ - Ca^{2+} exchanger, and other energy-dependent mechanisms. Oxygen, glucose, and energy restriction during cerebral ischemia rapidly results in increased cytoplasmic Ca^{2+} (25). If unchecked, excess Ca^{2+} can lead to enhanced phospholipase and protease activities, inducing irreversible catabolic processes and producing free radicals that activate multiple cell death pathways. Thus, there is an important adaptive advantage in upregulating the expression of Sur1-Trpm4 (i.e. the membrane depolarization induced by Ca^{2+} -mediated activation of Sur1-Trpm4 channels provides negative feedback that reduces the electrical driving force for inward Ca^{2+} flux and thereby acts to protect the cell

from excessive Ca^{2+}). However, sustained channel activity, as can be brought about by severe ATP depletion, results in continuous monovalent cation influx, converting an adaptive advantage into a maladaptive phenomenon that leads to cytotoxic edema and necrotic (oncotic) cell death (16).

The potential benefits of Sur1-Trpm4 channel blockade in stroke have been demonstrated in various studies. In a rat model of MCAo stroke, *Trpm4* gene suppression was associated with preserved vascular integrity, enhanced angiogenesis, reduced infarct volume, and improved functional recovery (13). A study using primary cultures of human umbilical vein endothelial cells showed that suppression of *Trpm4* by pharmacologic inhibition or by small interfering RNA protected cells against lipopolysaccharide-induced cell death (26). Sulfonylurea therapy via low-dose glibenclamide (a.k.a. glyburide), which binds to Sur1 and potentially inhibits the Sur1-Trpm4 channel, has been shown to confer protective effects, including reduced edema, cortical stroke volume, and overall mortality in various rodent stroke models (27–29). Moreover, sulfonylurea therapy in stroke patients with diabetes has been associated with improved neurologic function and reduced rates of symptomatic hemorrhagic transformation

FIGURE 7. Oncosis and membrane blebbing in Sur1-positive/Trpm4-positive cells in acute cerebral infarcts. Note the cytoplasmic vacuolization, membrane thickening, and irregularities present in endothelial cells of a small venule and a labeled neuron (A). Intravascular IgG is present within Sur1-negative microvessels (B) but is extravasated around Sur1-positive endothelium in infarcts (C). Similarly, intravascular IgG is present within Trpm4-negative microvessels (E) but is extravasated around Trpm4-positive endothelium in infarcts (F). Quantitative evaluation of IgG labeling in infarcted and noninfarcted regions of interest (ROI) revealed significant increases in perivascular IgG around Sur1-expressing and Trpm4-expressing versus nonexpressing vessels (D, G). Channel expression in microvessels is also associated with early hemorrhagic transformation (H), perivascular TNF labeling (I), and inflammation (J). ** $p < 0.01$. Original magnification: (A) 100×; (B, C, E, F, H–J) 40×. Scale bar = 10 μ m. Green/FITC, Trpm4, or IgG; red/CY3, Sur1, IgG, or TNF or myeloperoxidase; DAPI, blue. Images shown are from Cases 3 and 6.

and death relative to patients with diabetes who were managed without sulfonylurea agents (30,31). In a pilot study, stroke patients treated with RP-1127 (glyburide formulated for intravenous infusion) showed improved clinical outcomes compared with historical controls (30). The current study further supports the hypothesis that Sur1 coassociates with Trpm4 to form functional Sur1-Trpm4 channels in human cerebral ischemia and suggests that channel expression is associated with postischemic blood-brain barrier disruption and neuroinflammation. Because a constitutive function of this channel has not been identified in normal brain and because both *Abcc8* and *Trpm4* knockout mice exhibit near-normal phenotypes, pharmacologic inhibition of the Sur1-Trpm4 channel may represent a promising novel therapeutic strategy for patients sustaining focal cerebral infarction.

Because of an aging population, the absolute number of stroke events is projected to increase in the next 2 decades (32); thus, management of stroke patients remains a major clinical challenge. Affected patients are at high risk for progressive neurologic deterioration and death caused by malignant cerebral edema. Although researchers have made important progress in understanding the pathophysiology of stroke in recent years, specific molecular mechanisms involved in postischemic cell death remain relatively ill defined. Elucidation of these mechanisms is necessary to optimize outcomes for patients sustaining focal cerebral infarction. The identification of new pharmacotherapies with extended therapeutic time windows remains a critical goal in medicine. The current study is limited to examination of cerebral infarcts originating from stroke patients with poor outcome (i.e. death). Nonetheless, in light of recent data (14–16,22,33–35), these data suggest an important role for the Sur1-Trpm4 channel in the pathophysiology of postischemic cell death and implicates pharmacologic blockade of the Sur1-Trpm4 channel as a possible novel therapeutic strategy for mitigating neuronal loss and malignant cerebral edema in patients sustaining large territorial cerebral infarction.

ACKNOWLEDGMENT

We thank the National Institute of Child Health and Human Development Brain and Tissue Bank for Developmental Disorders at the University of Maryland for providing human tissues.

REFERENCES

- Sacco RL, Kasner SE, Broderick JP, et al. An updated definition of stroke for the 21st century: A statement for healthcare professionals from the American Heart Association/American Stroke Association. *Stroke* 2013;44:2064–89
- Go AS, Mozaffarian D, Roger VL, et al. Executive summary: Heart disease and stroke statistics—2013 update: A report from the American Heart Association. *Circulation* 2013;127:143–52
- Truelsen T, Begg S, Mathers C. The global burden of cerebrovascular disease. Available at: http://www.who.int/healthinfo/statistics/bod_cerebrovascular_diseases_stroke.pdf. Accessed December 30, 2012
- Adeoye O, Hornung R, Khatri P, et al. Recombinant tissue-type plasminogen activator use for ischemic stroke in the United States: A doubling of treatment rates over the course of 5 years. *Stroke* 2011;42:1952–55
- Jauss M, Schutz HJ, Tanislav C, et al. Effect of daytime, weekday and year of admission on outcome in acute ischaemic stroke patients treated with thrombolytic therapy. *Eur J Neurol* 2010;17:555–61
- Kleindorfer D, Lindsell CJ, Brass L, et al. National US estimates of recombinant tissue plasminogen activator use: ICD-9 codes substantially underestimate. *Stroke* 2008;39:924–28
- Singer OC, Hamann GF, Misselwitz B, et al. Time trends in systemic thrombolysis in a large hospital-based stroke registry. *Cerebrovasc Dis* 2012;33:316–21
- Lees KR, Bluhmki E, von Kummer R, et al. Time to treatment with intravenous alteplase and outcome in stroke: An updated pooled analysis of ECASS, ATLANTIS, NINDS, and EPITHET trials. *Lancet* 2010;375:1695–703
- Nilius B, Owsianik G. The transient receptor potential family of ion channels. *Genome Biol* 2011;12:218
- Mathar I, Jacobs G, Kecskes M, et al. TRPM4. *Handb Exp Pharmacol* 2012;222:461–87
- Vennekens R, Nilius B. Insights into TRPM4 function, regulation and physiological role. *Handb Exp Pharmacol* 2007;179:269–85
- Gerzanich V, Woo SK, Vennekens R, et al. De novo expression of Trpm4 initiates secondary hemorrhage in spinal cord injury. *Nat Med* 2009;15:185–91
- Loh KP, Ng G, Yu CY, et al. TRPM4 inhibition promotes angiogenesis after ischemic stroke. *Pflugers Arch* 2014;466:563–76
- Tosun C, Kurland DB, Mehta R, et al. Inhibition of the Sur1-Trpm4 channel reduces neuroinflammation and cognitive impairment in subarachnoid hemorrhage. *Stroke* 2013;44:3522–28
- Woo SK, Kwon MS, Ivanov A, et al. The sulfonylurea receptor 1 (sur1)-transient receptor potential melastatin 4 (trpm4) channel. *J Biol Chem* 2013;288:3655–67
- Simard JM, Woo SK, Gerzanich V. Transient receptor potential melastatin 4 and cell death. *Pflugers Arch* 2012;464:573–82
- Simard JM, Woo SK, Schwartzbauer GT, et al. Sulfonylurea receptor 1 in central nervous system injury: A focused review. *J Cereb Blood Flow Metab* 2012;32:1699–717
- Schattling B, Steinbach K, Thies E, et al. TRPM4 cation channel mediates axonal and neuronal degeneration in experimental autoimmune encephalomyelitis and multiple sclerosis. *Nat Med* 2012;18:1805–11
- Simard JM, Woo SK, Tsybalyuk N, et al. Glibenclamide-10-h treatment window in a clinically relevant model of stroke. *Transl Stroke Res* 2012;3:286–95
- Gerzanich V, Ivanov A, Ivanova S, et al. Alternative splicing of cGMP-dependent protein kinase I in angiotensin-hypertension: Novel mechanism for nitrate tolerance in vascular smooth muscle. *Circ Res* 2003;93:805–12
- Simard JM, Geng Z, Woo SK, et al. Glibenclamide reduces inflammation, vasogenic edema, and caspase-3 activation after subarachnoid hemorrhage. *J Cereb Blood Flow Metab* 2009;29:317–30
- Mehta RI, Ivanova S, Tosun C, et al. Sulfonylurea receptor 1 expression in human cerebral infarcts. *J Neuropathol Exp Neurol* 2013;72:871–83
- Patel AD, Gerzanich V, Geng Z, et al. Glibenclamide reduces hippocampal injury and preserves rapid spatial learning in a model of traumatic brain injury. *J Neuropathol Exp Neurol* 2010;69:1177–90
- Xu XZ, Moebius F, Gill DL, et al. Regulation of melastatin, a TRP-related protein, through interaction with a cytoplasmic isoform. *Proc Natl Acad Sci U S A* 2001;98:10692–97
- Kristian T, Siesjo BK. Calcium in ischemic cell death. *Stroke* 1998;29:705–18
- Becerra A, Echeverria C, Varela D, et al. Transient receptor potential melastatin 4 inhibition prevents lipopolysaccharide-induced endothelial cell death. *Cardiovasc Res* 2011;91:677–84
- Simard JM, Tsybalyuk N, Tsybalyuk O, et al. Glibenclamide is superior to decompressive craniectomy in a rat model of malignant stroke. *Stroke* 2010;41:531–37
- Simard JM, Chen M, Tarasov KV, et al. Newly expressed SUR1-regulated NC (Ca-ATP) channel mediates cerebral edema after ischemic stroke. *Nat Med* 2006;12:433–40
- Simard JM, Yurovsky V, Tsybalyuk N, et al. Protective effect of delayed treatment with low-dose glibenclamide in three models of ischemic stroke. *Stroke* 2009;40:604–9

30. Kunte H, Schmidt S, Eliasziw M, et al. Sulfonylureas improve outcome in patients with type 2 diabetes and acute ischemic stroke. *Stroke* 2007; 38:2526–30
31. Kunte H, Busch MA, Trostorf K, et al. Hemorrhagic transformation of ischemic stroke in diabetics on sulfonylureas. *Ann Neurol* 2012;72: 799–806
32. Kinlay S. Changes in stroke epidemiology, prevention, and treatment. *Circulation* 2011;124:e494–96
33. Sheth KN, Kimberly WT, Elm JJ, et al. Pilot study of intravenous glyburide in patients with a large ischemic stroke. *Stroke* 2014;45: 281–83
34. Simard JM, Kahle KT, Gerzanich V. Molecular mechanisms of microvascular failure in central nervous system injury—synergistic roles of NKCC1 and Sur1/Trpm4. *J Neurosurg* 2010;113:622–29
35. Zhang E, Liao P. Brain transient receptor potential channels and stroke. *J Neurosci Res* 2014. doi: 10.1002/jnr.23529